PARTICLE DATA GROUP NOTES PDG–93–06

8 December 1993

Energy loss in matter by heavy particles

Don Groom
Lawrence Berkeley Laboratory, Berkeley, CA 94720

1. Introduction

The 1992 *Review of Particle Properties* (RPP92) gives formulae for dE/dx, restricted dE/dx, and input parameters such as the effective ionization constant. Unfortunately this ionization constant is inconsistent with the accepted value, and the formulae cannot be used to calculate the same values of stopping power as are given in the graphs and (for minimum ionization) the tables. There are also some notational inconsistencies ($T_{\rm max}$ in Sec. 1 becomes $E_{\rm max}$ in Sec. 3, for instance) and many of the explanations leave much to be desired. The present study is directed toward removing these inconsistencies, and, along the way, revising the graphs and tabulated entries.

This note is not intended to be a review of the subject, but rather as a working paper to document and assist in the RPP revision. It is not of great literary merit.

Most of the notation is standard (like r_e for the classical electron radius), so for purposes of this note we relegate most definitions of the symbols to Appendix 1.

The standard canon of the subject begins with Bohr's classical treatment in 1913 [1]. We rely on the discussions by Rossi [2] and (especially) by Fano [3], and have gained a great deal of physical understanding from Jackson's treatment [4]. Barkas and Berger's tables have long been used (Ref. 5, hereafter Barkas64), and are the source of the minimum ionization values given in RPP92 and earlier RPP editions. However, most of the constants have since been improved. We have taken the ionization constants from Berger and Seltzer (Berger83, Ref. 6), which were adopted by the ICRU in 1984 (ICRU 37, Ref. 7) and have since been taken as standard. The density effect parameters for the elements are from Sternheimer, Berger, and Seltzer (1984) (Ste84, Ref. 8). The older values given in Sternheimer, Seltzer, and Berger (1982) (Ste82, Ref. 9) are used in EGS4 [10].

The newly-published ICRU 49 [11] updates the earlier discussions, particularly those concerning the shell and density effect corrections. We have used the tables in that report to check the present calculations at $T < 500$ MeV. The report also provides a comprehensive bibliography on the subject, as do Refs. 3 and 10.

This note is concerned with a region between $\beta\gamma = 0.13$ (a pion kinetic energy of 1.2 MeV) and $\beta\gamma \gtrsim 1000$ (a pion with several hundred GeV). Below the lower limit our shell correction fails, and in the region of the upper limit radiative effects become more important than ionization losses. The exact energy at which radiative effects dominate depends upon particle mass and stopping material.

The cross sections depend on the spin of the incident particle, and, in the case of the electrons, on identical particle considerations. Here we restrict ourselves to the spin-0 case, although the results can be applied to proton energy loss without sensible error.

2. Bethe-Bloch equation

We are concerned with the average energy loss as a high-energy massive charged particle passes through matter. By "high-energy" we mean that the velocity is high compared with that of atomic electrons (about αZ) and by massive we mean that the particle is not an electron—that is, it is a muon or a heavier particle. Most particles of interest have charge $\pm e$, but we leave open the possibility that the charge is ze.

At low energies nuclear recoil contributes to energy loss. At very high energies (above 100 GeV or so for a muon) radiative process contribute in a significant way and eventually dominate. Here we are concerned with the middle regime in which virtually all of the energy loss occurs via a large number of collisions with electrons in the medium. In this discussion the medium is taken as a pure element with atomic number Z and atomic mass A, but the restriction can easily be removed.

The mean energy loss rate ($-dE/dx$, or stopping power S) is therefore calculated by summing the contributions of all possible scatterings. These are normally scatterings from a lower to higher state, so that the particle loses a small amount of energy in each scattering. The kinetic energy of the scattered electron is T, and the magnitude of the 3-momentum transfer is q.

In the normal development, the matrix elements needed to find the cross sections are calculated using approximations appropriate to different T regions. The following are taken from Fano [3]. (We have replaced his recoil kinetic energy Q by T for consistency with other sources.)

1. *Low-T approximation.* Here $\hbar/q$ (roughly an impact parameter b) is large compared with atomic dimensions. The scattered electrons have kinetic energies up to some cutoff T_1, and the contribution to the stopping power is

$$S_1 = \frac{K}{2} z^2 \frac{Z}{A} \frac{1}{\beta^2} \left[\ln \frac{T_1}{I^2/2m_e c^2 \beta^2} + \ln \gamma^2 - \beta^2 \right] , \tag{1}$$

   where I is the appropriately weighted average excitation energy. The denominator $I^2/2m_e v^2$ in the first log term is the effective lower cutoff on the integral of dT/T. The first term comes from "longitudinal excitations" (the ordinary Coulomb potential), and the other two terms from transverse excitations.

   The low-T region is associated with large impact parameters and hence with long distances. Polarization of the medium can seriously reduce this contribution, particularly at high energies where the transverse extension of the incident particle's electric field becomes substantial. The correction is usually introduced by subtracting a separate term, δ, which is the subject of a later section of this report.

2. *Intermediate-T approximation.* In this region atomic excitation energies are not small compared with T, but, in contrast to the low-T region, transverse excitations can be neglected. It extends from T_1 to T_2, and the contribution to $-dE/dx$ is

$$S_2 = \frac{K}{2} z^2 \frac{Z}{A} \frac{1}{\beta^2} \left[\ln \frac{T_2}{T_1} \right] . \tag{2}$$

3. *High-T approximation.* In this region one can equate T with the energy given to the electron, *i.e.* neglect its binding energy. When the integration of the energy-weighted cross section is carried out between a lower limit T_2 (which is hopefully the same as in Eq. (2)) and an upper limit $T_{\rm upper}$, one obtains

$$S_3 = \frac{K}{2} z^2 \frac{Z}{A} \frac{1}{\beta^2} \left[\ln \frac{T_{\rm upper}}{T_2} - \beta^2 \frac{T_{\rm upper}}{T_{\rm max}} \right] . \tag{3}$$

Here $T_{\rm max}$ is the kinematic maximum possible electron recoil kinetic energy, given by

$$T_{\rm max} = \frac{2m_e c^2 \beta^2 \gamma^2}{1 + 2\gamma m_e/M + (m_e/M)^2} \ . \tag{4}$$

$T_{\rm upper}$ is normally equal to $T_{\rm max}$ (and will be treated this way at the conclusion of this section) but we will need the more general form in the discussion of restricted energy loss, below. In any case, $T_{\rm upper} \leq T_{\rm max}$.

In Fano's discussion, the low-energy approximation $T_{\rm max} \approx 2m_e c^2 \beta^2 \gamma^2$ is implicit. Accordingly, Eq. (3) is more closely related to Rossi's form (see his Eqns. 2.3.6 and 2.5.4).

The minimum T in this region, T_2, is much less than $m_e c^2$ but much larger than (any) electron's binding energy—a situation that becomes a little paradoxical for high-Z materials. The "shell correction" which corrects this problem is usually introduced as a term $-2C/Z$ inside the square brackets of Eq. (3).

The high-T region is associated with high-energy recoil particles, or δ rays. This is evident from an inspection of Eq. (3). For the usual case $T_{\rm upper} = T_{\rm max}$ the second term is virtually constant, while the first term rises as $\ln \gamma^2$. If the maximum transfer is limited to some $T_{\rm upper} < T_{\rm max}$, then the increase disappears.

In the above, we have implicitly assumed that one can find electron kinetic energies T_1 and T_2 at which the three regions join. This problem is discussed by Fano and others, and we ignore it here except to introduce the shell correction C/Z mentioned above.

When the three contributions are summed the intermediate T's cancel, and we get the usual Bethe-Bloch equation, which we choose to write in the following form:

$$-\frac{dE}{dx} = K z^2 \frac{Z}{A} \frac{1}{\beta^2} \left[\frac{1}{2} \ln \frac{2m_e c^2 \beta^2 \gamma^2 T_{\rm max}}{I^2} - \beta^2 - \frac{C}{Z} - \frac{\delta}{2} \right] \tag{5}$$

This function is plotted for $Z = 29$ (copper) in Fig. 1.

3. Maximum energy transfer to an electron

The maximum possible kinetic energy which can be imparted to an electron by a particle with mass M and momentum $M\beta\gamma$ is given by Eq. (4). It is usual to assume $2\gamma m_e/M << 1$ and replace this expression by its numerator, as is done in the version of the Bethe-Block equation given in RPP92. This is because a majority of the standard references date from the Bevatron days or are concerned with low-energy medical applications. In addition, computing the full expression once added complication. (It now seems remarkable that many of the older publications focused on simple analytic approximations to avoid implicit functions in expressions.) For pions in copper, the expressions with the approximate and exact forms for $T_{\rm max}$ result in energy loss rates which differ by 2% at 10 GeV and 6% at 100 GeV, as is shown in Fig. 2. For high-energy physics applications it seems important to use the complete expression to avoid known systematic errors at the 6% level. This is not always easy, as many of the references casually replace $T_{\rm max}$ by its approximate form.

At 100 GeV the maximum 4-momentum transfer to the electron is approaching 1 GeV, so that nucleon structure considerations are of possible importance. J. D. Jackson has investigated this problem [12]. He modified the cross sections with an appropriate form factor (using a ρ propagator),

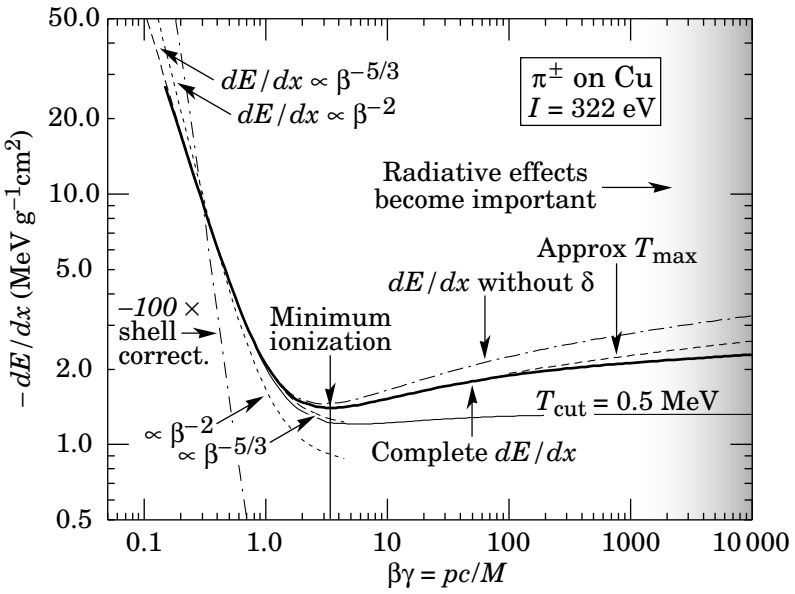

Figure 1: Energy loss rate in copper. The function without the density effect correction is also shown, as is the shell correction and two low-energy approximations.

and obtained a modified form for S_3 (see Eq. (3)). He was able to express the result as an additive term $f(2m_eT_{\max}/m_\rho^2)$ inside the square brackets of Eq. (5), where

$$f(x) = \ln(1+x) + \frac{1}{\gamma^2}\frac{x}{1+x} \tag{6}$$

For pions, his correction reaches only 0.4% at 200 GeV and 1.7% at 500 GeV. Since radiative energy losses dominate in most mid- to high-Z materials above a few hundred GeV, we are justified in neglecting structure effects.

4. Effective excitation energy

"The determination of the mean excitation energy is the principal non-trivial task in the evaluation of the Bethe stopping-power formula" [13].

Barkas64 defines an adjusted excitation energy $I_{\rm adj}$ such that the shell correction (next section) vanishes at high energy. Revised values for $I_{\rm adj}$ were published in Berger83 [6]. Many of these are experimental, based either upon direct stopping power measurements or "from moments of experimental dipole-oscillator-strength distributions or dielectric-response functions," whatever that means (Seltzer and Berger (1982) (Seltzer82, Ref. 13). These values were adopted as standard in ICRU 37 (1984) [7], and are repeated in ICRU 49 (1993) [11]. A useful comparison with other results is given in ICRU 49. They are also used in EGS4 [10], and should form the basis for any modern calculation. These are given in Appendix 2, and are shown (scaled by $1/Z$) in Fig. 3. The error estimates given in Appendix 2 are from Table 2 in Seltzer82.

For elements heavier than oxygen, $I_{\rm adj}/Z = 10 \pm 1$ eV, with bumps and valleys due to atomic shell effects. A variety of formulae have been proposed to obtain approximate values, including

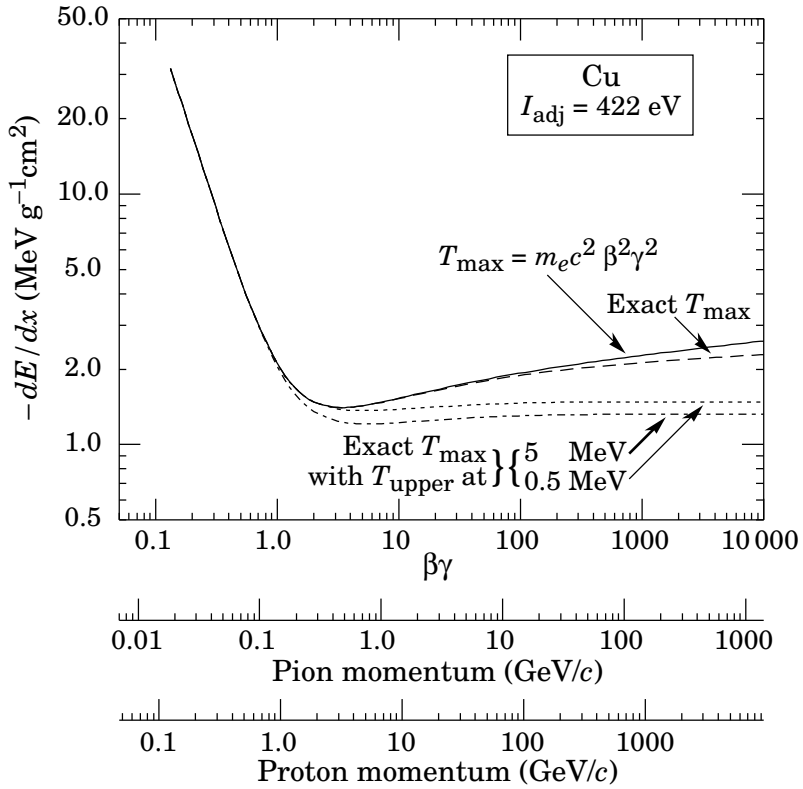

Figure 2: A comparison of exact and approximate forms for T_{max} for energy loss rates in copper. Also shown are restricted energy loss rates as given by Eq. (15) for two values of the cutoff energy.

that given by Barkas64 and the rather weird form ($I \approx 16Z^{-0.9}$ eV) given in RPP92 and earlier RPP editions. The latter is particularly bad, and its origins are lost in tradition. At this point in time, there seems little reason not to use the adopted values directly, since they are readily available from the tables in ICRU 49 (note error for scandium), from the references given above, and in the PEGS4 BLOCK DATA statements.

Values of I_{adj} are given for a wide variety of mixtures and compounds in Table 5.5 of Berger83 [6] and (especially) Seltzer84 [14].

5. Shell correction

Shell corrections become important only at the lowest energies. The function given in Barkas64 scales approximately as $(\beta\gamma)^{-3.5}$, and for copper reaches 1% at $\beta\gamma = 0.3$ (kinetic energy 6 MeV for a pion). The correction is therefore not of much interest in high-energy physics applications, except possibly for range calculations. We include it here because it is usually done, and because it is not hard. It is probably best not to include it in the Bethe-Bloch equation for RPP94.

As was mentioned, the shell correction does not quite vanish in the high-energy limit. Accordingly, one adjusts both I and C so that C_{adj} vanishes at high energies, although this point is not stressed in recent publications. Good treatments are given in sources such as ICRU 49, but for our purposes it is sufficient to used the older Barkas64 treatment, which suggests the analytic

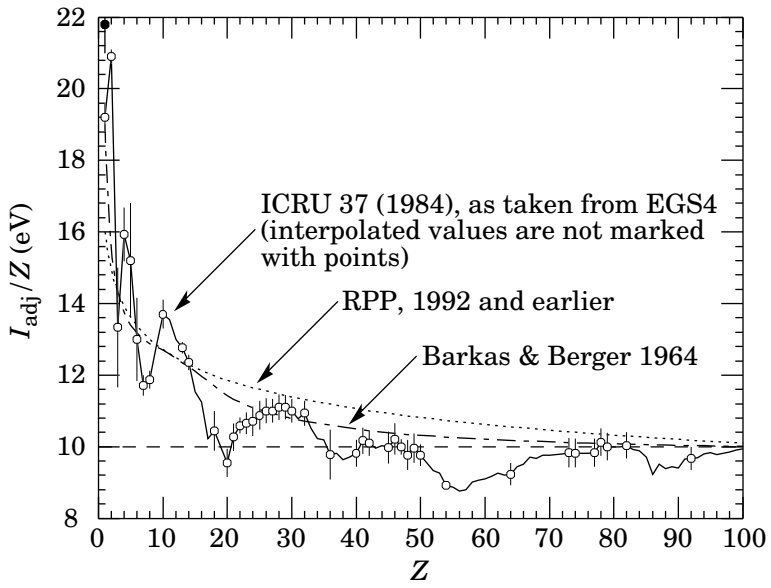

Figure 3: Excitation energies (divided by Z) as adopted by the ICRU [7]. Those based on measurement are shown by points with error flags; the interpolated values are simply joined. The solid point is for liquid H_2; the open point at 19.2 is for H_2 gas. Also shown are curves based on the approximate formulae of Barkas64 [5] and RPP92, which should be replaced for modern usage by the tabulated values. A machine-readable array may be found in the EGS4 BLOCK DATA statements [10].

approximation

$$\begin{aligned} C_{\rm adj} = &\left(0.422377\eta^{-2} + 0.0304043\eta^{-4} - 0.00038106\eta^{-6}\right) \times 10^{-6} I_{\rm adj}^2 \\ &+ \left(3.858019\eta^{-2} - 0.1667989\eta^{-4} + 0.00157955\eta^{-6}\right) \times 10^{-9} I_{\rm adj}^3 \ , \end{aligned} \tag{7}$$

where $\eta = \beta\gamma$ and $I_{\rm adj}$ is in eV. This form is valid only for $\eta > 0.13$ ($T = 1.2$ MeV for a pion).

6. Density effect correction

As the particle energy increases its electric field flattens and extends, so that the distant-collision part of dE/dx (Eq. (1) increases as $\ln\beta\gamma$. However, real media become polarized, limiting this extension and effectively truncating this part of the logarithmic rise. This "density effect" has been extensively treated over the years; see Refs. 8, 10, and 15, and references therein. At very high energies,

$$\delta/2 \to \ln\left(\hbar\omega_p/I\right) + \ln\beta\gamma - 1/2 \ , \tag{8}$$

where $\delta/2$ is the correction introduced in Eq. (5) and $\hbar\omega_p$ is the plasma energy:

$$\hbar\omega_p = \sqrt{4\pi N_e r_e^3}\ m_e c^2/\alpha = 28.816\sqrt{\rho\,\langle Z/A\rangle}\ \text{eV} \tag{9}$$

Here N_e is the electron density, and in the second form the material density ρ is in g cm^{-3}. A comparison with Eq. (5) shows that dE/dx grows as $\ln\beta\gamma$ rather than $\ln\beta^2\gamma^2$, and that the mean

excitation energy I is replaced by the plasma energy $\hbar\omega_p$. The effect of the density correction is shown in Fig. 1.

At some low energy the density effect is insignificant, and at some high energy it is sufficiently described by the asymptotic form given in Eq. (8). Sternheimer has proposed the following parameterization, which obviously dates from the days of log tables:

$$\delta = \begin{cases} 2\,(\ln 10)\,x - \overline{C} & \text{if } x \geq x_1; \\ 2\,(\ln 10)\,x - \overline{C} + a\,(x_1 - x)^k & \text{if } x_0 \leq x < x_1; \\ 0 & \text{if } x < x_0 \text{ (nonconductors)}; \\ \delta_0 10^{2(x - x_0)} & \text{if } x < x_0 \text{ (conductors)}\ , \end{cases} \tag{10}$$

where $x = \log_{10}\eta = \log_{10}(p/Mc)$. $\overline{C}$ is obtained by equating the high-energy case of Eq. (10) with the limit of Eq. (8). The other parameters are adjusted to give a best fit to the results of detailed calculations for momenta below $Mc\exp(x_1)$. Note that $\overline{C}$ is the negative of the C used in earlier publications. A variety of different parameters are available. In some cases these result from a different fitting procedure having been used with the same model, and the resulting δ is not sensibly different. For elements the PEGS4 data blocks [10] use the values from Ste82 [9]. These have since been superceded by the values in Ste84 [8], which are also given in Appendix 2. The agreement with more detailed calculations or with other parameter sets is usually at the 0.5% level [14].

Seltzer84 [14] extends this to nearly 200 compounds, albeit in the context of $e^{\pm}$ energy loss, and give the density effect corrections in terms of coefficients $b_0, \ldots, b_4,\ k$. The translation table from these coefficients to the Sternheimer coefficients follows:

$$\begin{aligned} \overline{C} &= b_1 - b_0 + 1 \\ \delta_0 &= \eta_0^2 b_4 \\ x_1 &= b_3/2\ln 10 \quad \text{(or calculate from } T_1\text{)} \\ k &= k \end{aligned} \tag{11}$$

Instead of x_0 and x_1, Seltzer84 gives the related electron kinetic energies T_0 and T_1. Following their notation, $\tau \equiv T/m_e c^2 = \gamma - 1$, so $\eta \equiv \beta\gamma = \sqrt{\tau(\tau+2)}$, and $x = \ln\eta/\ln 10 = \log_{10}\eta$.

7. Comparison of results

One of the original motivations for this study was the observation that the formulae given in the RPP "Passage of Particles through Matter" section could not be used to produce the minimum ionization values given in the "Atomic and Nuclear Properties of Materials" table. The values given in this Table were evidently taken from Berger64, and are based on constants long since superceded. In particular, the values for minimum ionization given in ICRU 49 are about 3% lower, largely because of the improved density effect correction. Results for pions in copper are given in Table 1. It is disturbing that our results disagree in the 4th place, given that identical constants (including the old value for the pion mass) were used, but we regard the agreement as satisfactory. Similarly, we seem able to reproduce the ICRU 49 numbers in spite of more naïve shell and density effect corrections.

Table 1: Comparison of stopping power results for pions in copper. The minimum occurs at $\gamma = 3.50$–3.55, depending upon the density effect constants.

Source	Min ion.	10 MeV	100 MeV	5 GeV
RPP92 Properties of Materials table	1.44	—	—	—
Barkas64 [5]	1.4364	6.5274	1.7162	1.7816
Present calc, Barkas64 constants	1.4373	6.5251	1.7165	1.7846
ICRU 49 [11]	1.402	6.471	1.686	—
Present calc, EGS4 manual constants [10]	1.4018	6.4898	1.6870	1.7434
Present calc, Ste84 constants [8]	1.4026	6.4825	1.6877	1.7434

8. Energy loss in compounds and mixtures

It is usual to think of a compound or mixture as made up of thin layers of the pure elements in the right proportion (Bragg additivity). Let n_j be the number of the jth kind of atom in a compound (it need not be an integer for a mixture), and w_j its weight fraction:

$$w_j = n_j A_j \Big/ \sum_k n_k A_k \tag{12}$$

Then

$$\left\langle \frac{dE}{dx} \right\rangle = \sum_j w_i \left. \frac{dE}{dx} \right|_j \tag{13}$$

When the Bethe-Block equation is inserted and the Z-dependent terms sorted out, we find that this is equivalent to a single material with

$$\begin{aligned}
\left\langle \frac{Z}{A} \right\rangle &= \sum_j w_j \frac{Z_j}{A_j} &&= \sum_j n_j Z_j \Big/ \sum_j n_j A_j \\
\ln \langle I \rangle &= \sum_j w_j \left(Z_j/A_j\right) \ln I_j \Big/ \sum_j w_j \left(Z_j/A_j\right) &&= \sum_j n_j Z_j \ln I_j \Big/ \sum_j n_j Z_j \\
\langle C/Z \rangle &= \sum_j w_j \left(Z_j/A_j\right) \left(C_j/Z_j\right) I_j \Big/ \sum_j w_j \left(Z_j/A_j\right) &&= \sum_j n_j Z_j \left(C_j/Z_j\right) \Big/ \sum_j n_j Z_j \\
\langle \delta \rangle &= \sum_j w_j \left(Z_j/A_j\right) \delta_j \Big/ \sum_j w_j \left(Z_j/A_j\right) &&= \sum_j n_j Z_j \delta_j \Big/ \sum_j n_j Z_j
\end{aligned} \tag{14}$$

Within a scale factor which cancels, the n_j are the same as the number fractions p_j which the EGS4 manual uses in defining $\langle I \rangle$.

However, there are pitfalls:

1. Since the electrons in a compound are more tightly bound than in the constituent elements, the effective I_j are in general higher than those of the constituent elements. But exceptions are provided by diatomic gases and by metals in metallic alloys or compounds. The right way to to it is to do it right, but Berger and Seltzer discuss ways to extend the Bragg additivity rule:

   1.1. For a select list of materials (carbon and some common gases), they propose alternate mean excitation energies in their Table 5.1 (or Table 6 in Seltzer82).

   1.2. For other elements, the excitation is multiplied by 1.13 before calculation of the mean (the "13% rule"). Although it is is not said, it would seem sensible to apply this rule in the case of a tightly-bound material such as CsI, and not apply it in the case of a metallic compound like Nb_3Sn.

   1.3. Both are superceded by experimental numbers when available, as in the case of SiO_2.

   Since none of this is mentioned in the EGS4 manual, a certain degree of confusion results if one tries to use its algorithm to compute the values in Table 2.13.2.

   Experimental excitation energies are now available for several hundred materials [13,14], and programs like FLUKA92 override EGS4 defaults to use them.

2. The density effect is just that, and it makes little sense to use the above expression. Default constants for a large number of common materials are available in Seltzer84 [14]. If the material of interest is not available in these tables, then the algorithm given by Sternheimer and Peierls [15] should be used. Their recipe is given more succinctly in the EGS4 manual [10], but one should use our Eq. (9).

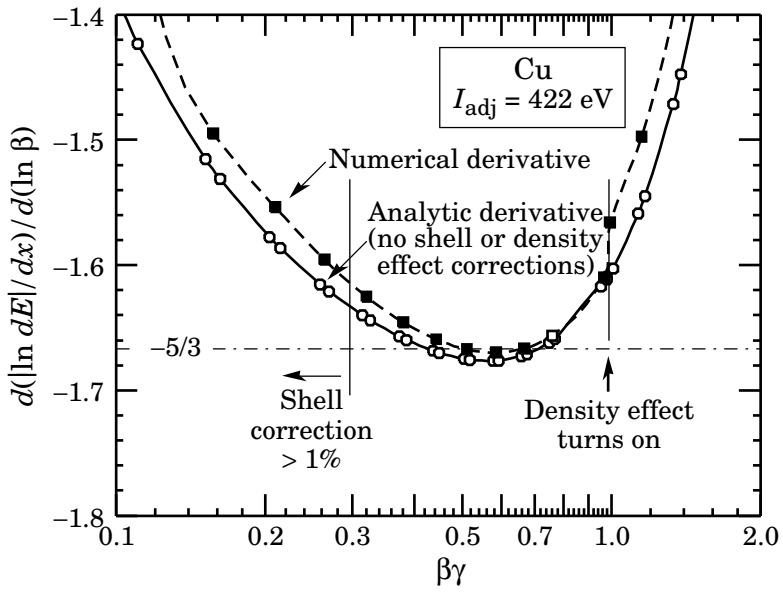

Figure 4: The logarithmic derivative of $|dE/dx|$ with respect to β. Analytic derivatives were calculated at the pairs of abscissas shown by the open points, using Eq. (5) without the shell or density corrections; values including these corrections were differenced to obtain the solid points. The Sternheimer form for the density correction has a discontinuous derivative at $x_0 = \log_{10} \beta\gamma$; the metallic correction for smaller x's was not used in this calculation. $|dE/dx| \propto \beta^{-5/3}$ is shown in Fig. 1, along with the $|dE/dx| \propto \beta^{-2}$ form described in most references.

9. Low-energy behavior

It is often stated that at low energies ($\ln\gamma \approx 0$), dE/dx scales as $1/v^2$. This result is obtained by assuming that the square bracketed quantity in Eq. (5) varies slowly enough that it can be considered to be constant. We have computed the derivative $d(\ln|dE/dx|)/d(\ln\beta)$ by two methods: analytically, ignoring the density effect and shell corrections, and numerically, using the complete Bethe-Block equation. For no value of β is the slope anywhere near this steep.

These results are shown in Fig. 4. As can be seen, the slope reaches a minimum value of about -1.68 at $\beta\gamma = 0.6$. As it turns out, $|dE/dx| \propto \beta^{-5/3}$ provides a very good fit to the data in the low-energy region. A curve of this form is shown in Fig. 1. The usual β^{-2} is shown for comparison; it fits nowhere and crosses the exact function with a very different slope. (I actually saw the slope given as $-5/3$ in some reference or another, but can no longer find it.)

10. Restricted energy loss and δ rays

We have commented that the increase of the high-T part of the stopping power is due to the increasing production of energetic secondaries; that is, to the increase of $T_{\rm max}$. In some experimental situations these are separately observable (bubble chambers, cloud chambers, emulsions, drift chambers [single hits adjacent to tracks], *etc.*), and are called δ rays. In other situations (thin scintillators) the δ rays can escape, so that deposited energy is not the same as energy lost in the material.

In a more typical situation (*e.g.* in the sensitive layers of a calorimeter), there is an equilibrium between energy carried into the sensitive layer by δ rays produced in the absorber and energy carried out by δ rays produced in the sensitive region. Even for a layer deep enough in the calorimeter for equilibrium to exist, these may not be identical. A GEANT calculation by C. Hearty [16] of energy deposit by a 10 GeV muon going through a lead-scintillator stack (3 mm plates and scintillators) shows an increase of 11% in the signals over the first $\sim$8 radiation lengths, as the δ-ray equilibrium is established. The use of Eq. (15) does not provide a complete description of the signal in the first ("naked") scintillator, since (a) $T_{\rm cut}$ is a function of depth in the scintillator plate, and (b) at least some of the δ-ray energy is deposited, again as function of the depth in which the δ ray are produced. So far, we have not found a good way to estimate the energy deposit.

In Monte Carlo simulations, one often wishes to treat the energy lost to a myriad of minor collisions as continuous, while treating the rare hard collision losses as random processes. In any case, it is of interest to calculate the "restricted" energy loss rate, that is, with the loss in a single collision limited to some energy $T_{\rm cut} < T_{\rm max}$. In the formula in RPP92 and earlier editions, this is done, at least in essence, by replacing $T_{\rm max}$ by the constant $T_{\rm cut}$ in the logarithmic term and neglecting it elsewhere. This is wrong; among other things, it results in a larger energy loss rate for $T_{\rm cut} > T_{\rm max}$ (at low energies) than would be the case without the cutoff.

The problem is straightforward: Use Eq. (3), but choose $T_{\rm upper}$ as the lesser of $T_{\rm cut}$ and $T_{\rm max}$. Eq. (5) then becomes

$$-\left.\frac{dE}{dx}\right|_{T<T_{\rm cut}} = Kz^2\frac{Z}{A}\frac{1}{\beta^2}\left[\frac{1}{2}\ln\frac{2m_ec^2\beta^2\gamma^2T_{\rm upper}}{I^2} - \frac{1}{2}\beta^2\left(1+\frac{T_{\rm upper}}{T_{\rm max}}\right) - \frac{C}{Z} - \frac{\delta}{2}\right] \qquad (15)$$

where $T_{\rm upper} = {\rm MIN}(T_{\rm cut}, T_{\rm max})$. This form agrees with the equation in RPP92 for $T_{\rm cut} << T_{\rm max}$ but smoothly joins the normal Bethe-Bloch function for $T_{\rm cut} > T_{\rm max}$.

RPP92 and earlier editions also give a formula for the number distribution of δ rays per unit length as a function of energy. When this expression is multiplied by T (to convert number to energy) and integrated over T, one obtains

$$-\left.\frac{dE}{dx}\right|_{\delta\ {\rm rays}} = Kz^2\frac{Z}{A}\frac{1}{\beta^2}\int_{T_{\rm cut}}^{T_{\rm max}}\frac{F(T)}{T}dT\ . \qquad (16)$$

According to Rossi (Eq. 2.3.6), $F(T) = (1-\beta^2T/T_{\rm max})$ for spin-0 particles. The integral thus yields the difference between the complete (Eq. (5)) and restricted (Eq. (15)) energy loss rates.

Appendix 1: Symbols used in this report

Symbol	Definition	Units or Value
v	Incident particle velocity	
c	Velocity of light	
β	v/c	
γ	$1/\sqrt{1-\beta^2}$	
α	Fine structure constant	$1/137.035\,989\,5(61)$
η	$\beta\gamma$	(Rossi's η is our T_2)
M	Incident particle mass	MeV/c^2
E	Incident particle energy γMc^2	MeV
T	Kinetic energy	MeV
q	Magnitude of 3-momentum transfer to electron in medium	MeV/c
$m_e c^2$	Electron mass $\times c^2$	0.510 999 06(15) MeV
e	Electronic charge	
r_e	Classical electron radius $e^2/4\pi\epsilon_0 m_e c^2$	2.817 940 92(38) fm
N_A	Avocado's number	$6.022\,136\,7(36) \times 10^{23}$ mol^{-1}
z	Charge of incident particle/e	
Z	Atomic number of medium	
A	Atomic mass of medium	g mol^{-1}
K/A	$4\pi N_A r_e^2 m_e c^2/A$	0.307 075 MeV g^{-1} cm^2 for $A = 1$ g mol^{-1}
Rossi's C	$\pi N_A (Z/A) r_e^2 = K(Z/A)/4m_e c^2$	0.150 Z/A g^{-1}cm^2
C/Z	Shell correction	(This is not Rossi's C)
δ	Density effect correction	

References

1. N. Bohr, Phil. Mag. **25**, 10 (1913).
2. B. Rossi, *High Energy Particles*, Prentice-Hall, Inc., Englewood Cliffs, NJ, 1952.
3. U. Fano, Ann. Rev. Nucl. Sci. **13**, 1 (1963).
4. J. D. Jackson, *Classical Electrodynamics* John Wiley & Sons, NY (1962).
5. W. H. Barkas and M. J. Berger, *Tables of Energy Losses and Ranges of Heavy Charged Particles*, NASA-SP-3013 (1964).
6. M. J. Berger and S. M. Seltzer, "Stopping Powers and Ranges of Electrons and Positrons" (2nd edition), U. S. Department of Commerce Report NBSIR 82-2550-A (1983).
7. ICRU Report 37, "Stopping Powers for Electrons and Positrons," International Commission on Radiation Units and Measurements, Washington, DC (1984).
8. R. M. Sternheimer, M. J. Berger, and S. M. Seltzer, Atomic Data and Nuclear Data Tables **30**, 261–271 (1984).
9. R. M. Sternheimer, S. M. Seltzer, and M. J. Berger, Phys. Rev. **B26**, 6067–6076 (1982).
10. W.R. Nelson, H. Hirayama, and D. W. O. Rogers, "The EGS4 Code System," SLAC-265, Stanford Linear Accelerator Center (Dec. 1985).

Appendix 2: Data needed to calculate dE/dx

Atomic constants, densities, ionization constants, and Sternheimer coefficients for the chemical elements. The ionization constants and Sternheimer coefficients are from Ref. 8, while the errors in the ionization constants are from Ref. 6. The liquid H_2 numbers are for bubble chamber conditions; the density at the boiling point at 1 atm is 0.0708 g cm^{-3}. If there is no characteristic terrestrial composition of an element with no stable isotopes, the atomic mass of the most stable is given (see the Periodic Table in RPP94). A density given below is sometimes the average over different allotropes (as with P and Se); it is not corrected because it is the one used to calculate the Sternheimer coefficients. Gas densities are evaluated at 1 atm and 20° C. Parentheses around ionization constants indicate interpolated values.

Material	Z	A g mol^{-1}	ρ g cm^{-3}	$I_{\rm adj}$ eV	$\overline{C}$	x_0	x_1	a	k	δ_0
H_2 gas	1	1.00797	8.37×10^{-5}	19.2 ±0.4	9.5835	1.8639	3.2718	0.1409	5.7273	0.00
H_2 liq (BC)	1	1.00797	6.00×10^{-2}	21.8 ±0.4	3.2632	0.4759	1.9215	0.1348	5.6249	0.00
He gas	2	4.0026	1.66×10^{-4}	41.8 ±0.8	11.1393	2.2017	3.6122	0.1344	5.8347	0.00
Li	3	6.939	0.534	40 ±5	3.1221	0.1304	1.6397	0.9514	2.4993	0.14
Be	4	9.0122	1.848	63.7 ±3	2.7847	0.0592	1.6922	0.8039	2.4339	0.14
B	5	10.811	2.37	76 ±8	2.8477	0.0305	1.9688	0.5622	2.4512	0.14
C graphite	6	12.01115	2.265	78 ±7	2.8680	−0.0178	2.3415	0.2614	2.8697	0.12
C graphite	6	12.01115	2.0	78 ±7	2.9925	−0.0351	2.4860	0.2024	3.0036	0.10
C graphite	6	12.01115	1.7	78 ±7	3.1550	0.0480	2.5387	0.2076	2.9532	0.14
N_2 gas	7	14.0067	1.17×10^{-3}	82 ±2	10.5400	1.7378	4.1323	0.1535	3.2125	0.00
O_2 gas	8	15.9994	1.33×10^{-3}	95 ±2	10.7004	1.7541	4.3213	0.1178	3.2913	0.00
F_2 gas	9	18.9984	1.58×10^{-3}	(115 ±10)	10.9653	1.8433	4.4096	0.1108	3.2962	0.00
Ne gas	10	20.183	8.39×10^{-4}	137 ±4	11.9041	2.0735	4.6421	0.0806	3.5771	0.00
Na	11	22.9898	0.971	(149 ±10)	5.0526	0.2880	3.1962	0.0777	3.6452	0.08
Mg	12	24.312	1.74	(156 ±10)	4.5297	0.1499	3.0668	0.0816	3.6166	0.08
Al	13	26.9815	2.699	166 ±2	4.2395	0.1708	3.0127	0.0802	3.6345	0.12
Si	14	28.088	2.33	173 ±3	4.4351	0.2014	2.8715	0.1492	3.2546	0.14
P	15	30.9738	2.2	(173 ±15)	4.5214	0.1696	2.7815	0.2361	2.9158	0.14
S	16	32.064	2.000	(180 ±15)	4.6659	0.1580	2.7159	0.3399	2.6456	0.14
Cl_2 gas	17	35.453	2.99×10^{-3}	(174 ±15)	11.1421	1.5555	4.2994	0.1985	2.9702	0.00
Ar gas	18	39.948	1.66×10^{-3}	188 ±10	11.9480	1.7635	4.4855	0.1971	2.9618	0.00
K	19	39.102	0.862	(190 ±15)	5.6423	0.3851	3.1724	0.1983	2.9233	0.10
Ca	20	40.08	1.55	191 ±8	5.0396	0.3228	3.1191	0.1564	3.0745	0.14
Sc	21	44.956	2.989	216 ±8	4.6949	0.1640	3.0593	0.1575	3.0517	0.10
Ti	22	47.9	4.54	233 ±5	4.4450	0.0957	3.0386	0.1566	3.0302	0.12
V	23	50.942	6.11	245 ±7	4.2659	0.0691	3.0322	0.1544	3.0163	0.14
Cr	24	51.998	7.18	257 ±10	4.1781	0.0340	3.0451	0.1542	2.9896	0.14
Mn	25	54.938	7.44	272 ±10	4.2702	0.0447	3.1074	0.1497	2.9796	0.14
Fe	26	55.847	7.874	286 ±9	4.2911	−0.0012	3.1531	0.1468	2.9632	0.12
Co	27	58.9332	8.90	297 ±9	4.2601	−0.0187	3.1790	0.1447	2.9502	0.12
Ni	28	58.71	8.902	311 ±10	4.3115	−0.0566	3.1851	0.1650	2.8430	0.10
Cu	29	63.54	8.960	322 ±10	4.4190	−0.0254	3.2792	0.1434	2.9044	0.08
Zn	30	65.37	7.133	330 ±10	4.6906	0.0049	3.3668	0.1471	2.8652	0.08
Ga	31	69.72	5.904	(334 ±20)	4.9353	0.2267	3.5434	0.0944	3.1314	0.14
Ge	32	72.59	5.323	350 ±11	5.1411	0.3376	3.6096	0.0719	3.3306	0.14
As	33	74.9216	5.73	(347 ±25)	5.0510	0.1767	3.5702	0.0663	3.4176	0.08
Se	34	78.96	4.5	(348 ±30)	5.3210	0.2258	3.6264	0.0657	3.4317	0.10
Br_2 gas	35	79.808	7.07×10^{-3}	(343 ±30)	11.7307	1.5262	4.9899	0.0633	3.4670	0.00
Br_2 liq	35	79.808	3.120	(357 ±30)	—	—	—	—	—	0.00

Appendix 2: Continued

Material	Z	A g mol^{-1}	ρ g cm^{-3}	$I_{\rm adj}$ eV	$\overline{C}$	x_0	x_1	a	k	δ_0
Kr	36	83.8	3.48×10^{-3}	352 ±25	12.5115	1.7158	5.0748	0.0745	3.4051	0.00
Rb	37	85.47	1.532	(363 ±30)	6.4776	0.5737	3.7995	0.0726	3.4177	0.14
Sr	38	87.62	2.540	(366 ±30)	5.9867	0.4585	3.6778	0.0716	3.4435	0.14
Y	39	88.905	4.469	(379 ±30)	5.4801	0.3608	3.5542	0.0714	3.4585	0.14
Zr	40	91.22	6.506	393 ±15	5.1774	0.2957	3.4890	0.0718	3.4533	0.14
Nb	41	92.906	8.570	417 ±15	5.0141	0.1785	3.2201	0.1388	3.0930	0.14
Mo	42	95.94	10.220	424 ±15	4.8793	0.2267	3.2784	0.1053	3.2549	0.14
Tc 43	43	99.	11.500	(428 ±35)	4.7769	0.0949	3.1253	0.1657	2.9738	0.14
Ru	44	101.07	12.410	(441 ±35)	4.7694	0.0599	3.0834	0.1934	2.8707	0.14
Rh	45	102.905	12.410	449 ±20	4.8008	0.0576	3.1069	0.1920	2.8633	0.14
Pd	46	106.4	12.020	470 ±20	4.9358	0.0563	3.0555	0.2418	2.7239	0.14
Ag	47	107.87	10.500	470 ±10	5.0630	0.0657	3.1074	0.2458	2.6899	0.14
Cd	48	112.4	8.650	469 ±20	5.2727	0.1281	3.1667	0.2461	2.6772	0.14
In	49	114.82	7.310	488 ±20	5.5211	0.2406	3.2032	0.2388	2.7144	0.14
Sn	50	118.69	7.310	488 ±15	5.5340	0.2879	3.2959	0.1869	2.8576	0.14
Sb	51	121.75	6.691	(487 ±40)	5.6241	0.3189	3.3489	0.1665	2.9319	0.14
Te	52	127.6	6.240	(485 ±40)	5.7131	0.3296	3.4418	0.1382	3.0354	0.14
I_2 gas	53	126.9044	1.13×10^{-2}	(474 ±40)	—	—	—	—	—	0.00
I sol	53	126.9044	4.930	(491 ±40)	5.9488	0.0549	3.2596	0.2377	2.7276	0.00
Xe gas	54	131.3	5.49×10^{-3}	482 ±30	12.7281	1.5630	4.7371	0.2331	2.7414	0.00
Cs	55	132.905	1.873	(488 ±40)	6.9135	0.5473	3.5914	0.1823	2.8866	0.14
Ba	56	137.34	3.500	(491 ±40)	6.3153	0.4190	3.4547	0.1827	2.8906	0.14
La	57	138.91	6.154	(501 ±40)	5.7850	0.3161	3.3293	0.1859	2.8828	0.14
Ce	58	140.12	6.657	(523 ±40)	5.7837	0.2713	3.3432	0.1889	2.8592	0.14
Pr	59	140.907	6.710	(535 ±45)	5.8096	0.2333	3.2773	0.2326	2.7331	0.14
Nd	60	144.24001	6.900	(546 ±45)	5.8290	0.1984	3.3063	0.2353	2.7050	0.14
Pm 145	61	147.	7.220	(560 ±45)	5.8224	0.1627	3.3199	0.2428	2.6674	0.14
Sm	62	150.35001	7.460	(574 ±45)	5.8597	0.1520	3.3460	0.2470	2.6403	0.14
Eu	63	151.98	5.243	(580 ±50)	6.2278	0.1888	3.4633	0.2445	2.6245	0.14
Gd	64	157.25	7.900	591 ±20	5.8738	0.1058	3.3932	0.2511	2.5977	0.14
Tb	65	158.924	8.229	(614 ±55)	5.9045	0.0947	3.4224	0.2445	2.6056	0.14
Dy	66	162.5	8.550	(628 ±55)	5.9183	0.0822	3.4474	0.2466	2.5849	0.14
Ho	67	164.92999	8.795	(650 ±60)	5.9587	0.0761	3.4782	0.2464	2.5726	0.14
Er	68	167.25999	9.066	(658 ±60)	5.9521	0.0648	3.4922	0.2482	2.5573	0.14
Tm	69	168.93401	9.321	(674 ±60)	5.9677	0.0812	3.5085	0.2489	2.5469	0.14
Yb	70	173.03999	6.730	(684 ±65)	6.3325	0.1199	3.6246	0.2530	2.5141	0.14
Lu	71	174.97	9.840	(694 ±65)	5.9785	0.1560	3.5218	0.2403	2.5643	0.14
Hf	72	178.49001	13.310	(705 ±65)	5.7139	0.1965	3.4337	0.2292	2.6155	0.14
Ta	73	180.948	16.654	718 ±30	5.5262	0.2117	3.4805	0.1780	2.7623	0.14
W	74	183.85001	19.300	727 ±30	5.4059	0.2167	3.4960	0.1551	2.8447	0.14
Re	75	186.2	21.020	(736 ±70)	5.3445	0.0559	3.4845	0.1518	2.8627	0.08
Os	76	190.2	22.570	(746 ±70)	5.3083	0.0891	3.5414	0.1275	2.9608	0.10
Ir	77	192.2	22.420	757 ±30	5.3418	0.0819	3.5480	0.1269	2.9658	0.10
Pt	78	195.08	21.450	790 ±30	5.4732	0.1484	3.6212	0.1113	3.0417	0.12
Au	79	196.987	19.320	790 ±30	5.5747	0.2021	3.6979	0.0976	3.1101	0.14
Hg	80	200.59	13.546	(800 ±75)	5.9605	0.2756	3.7275	0.1101	3.0519	0.14
Tl	81	204.37	11.720	(810 ±75)	6.1365	0.3491	3.8044	0.0945	3.1450	0.14
Pb	82	207.19	11.350	823 ±30	6.2018	0.3776	3.8073	0.0936	3.1608	0.14
Bi	83	208.98	9.747	(823 ±80)	6.3505	0.4152	3.8248	0.0941	3.1671	0.14

Appendix 2: Continued

Material	Z	A g mol^{-1}	ρ g cm^{-3}	$I_{\rm adj}$ eV	$\overline{C}$	x_0	x_1	a	k	δ_0
Po 209	84	210.	9.320	(830 ±80)	6.4003	0.4267	3.8293	0.0928	3.1830	0.14
At 210	85	210.	1.000	(841 ±80)	—	—	—	—	—	0.14
Rn 222 gas	86	222.	9.07×10^{-3}	(794 ±80)	13.2839	1.5368	4.9889	0.2080	2.7409	0.00
Fr 223	87	223.	1.	(827 ±80)	—	—	—	—	—	0.14
Ra	88	226.	5.	(826 ±80)	7.0452	0.5991	3.9428	0.0880	3.2454	0.14
Ac	89	227.	10.07	(841 ±80)	6.3742	0.4559	3.7966	0.0857	3.2683	0.14
Th	90	232.0381	11.72	(847 ±80)	6.2473	0.4202	3.7681	0.0865	3.2610	0.14
Pa	91	231.03588	15.37	(878 ±80)	6.0327	0.3144	3.5079	0.1477	2.9845	0.14
U	92	238.0289	18.95	890 ±30	5.8694	0.2260	3.3721	0.1968	2.8171	0.14
Np	93	237.0482	20.25	(902 ±80)	5.8149	0.1869	3.3690	0.1974	2.8082	0.14
Pu 244	94	244.0642	19.84	(921 ±85)	5.8748	0.1557	3.3981	0.2042	2.7679	0.14
Am 243	95	243.0614	13.67	(934 ±85)	6.2813	0.2274	3.5021	0.2031	2.7615	0.14
Cm 247	96	247.07035	13.51	(939 ±85)	6.3097	0.2484	3.5160	0.2026	2.7579	0.14
Bk 247	97	247.07030	14.	(952 ±85)	6.2912	0.2378	3.5186	0.2019	2.7560	0.14
Cf 251	98	251.07958	—	(966 ±90)	—	—	—	—	—	0.14
Es 252	99	252.08295	—	(980 ±90)	—	—	—	—	—	0.14
Fm 257	100	257.0951	—	(994 ±90)	—	—	—	—	—	0.14

11. "Stopping Powers and Ranges for Protons and Alpha Particles," ICRU Report No. 41 (1993).

12. J. D. Jackson, "Effect of Form Factor on dE/dx from Close Collisions," Particle Data Group Note PDG-93-04 (19 October 1993) (unpublished).

13. S. M. Seltzer and M. J. Berger, Int. J. Appl. Radiat. **33**, 1189–1218 (1982).

14. S. M. Seltzer and M. J. Berger, Int. J. Appl. Radiat. **35**, 665–676 (1984). This paper corrects and extends the results of [13].

15. R. M. Sternheimer and R. F. Peierls, Phys. Rev. **B3**, 3681–3692 (1971).

16. C. Hearty, private communication (1993).